Available online at www.sciencedirect.com

ScienceDirect

Mendeleev Commun., 2023, **33**, 384–386

Mendeleev Communications

Synthesis and optical characteristics of 4-styrylpyridinium dyes and their conjugates with antibody

Anna S. Efimova,[a,b] Mariya A. Ustimova,[a] Margarita A. Maksimova,[a,c,d] Anastasya Yu. Frolova,[a,c] Vladimir I. Martynov,[c] Sergey M. Deyev,[c] Alexey A. Pakhomov,[a,c] Yurii V. Fedorov[a] and Olga A. Fedorova*[a,b]

[a] *A. N. Nesmeyanov Institute of Organoelement Compounds, Russian Academy of Sciences, 119334 Moscow, Russian Federation. E-mail: fedorova@ineos.ac.ru*
[b] *D. I. Mendeleev University of Chemical Technology of Russia, 125047 Moscow, Russian Federation*
[c] *M. M. Shemyakin–Yu. A. Ovchinnikov Institute of Bioorganic Chemistry, Russian Academy of Sciences, 117997 Moscow, Russian Federation*
[d] *Department of Chemistry, M. V. Lomonosov Moscow State University, 119991 Moscow, Russian Federation*

DOI: 10.1016/j.mencom.2023.04.027

Two new styryl-type dyes modified with the succinimide ester group were prepared for conjugation with antibodies. The optical characteristics of the obtained compounds in different solvents were studied, and the solvatochromic properties of these dyes were revealed. The applicability of the dyes as protein labels was demonstrated in cyto-fluorometry and fluorescence microscopy.

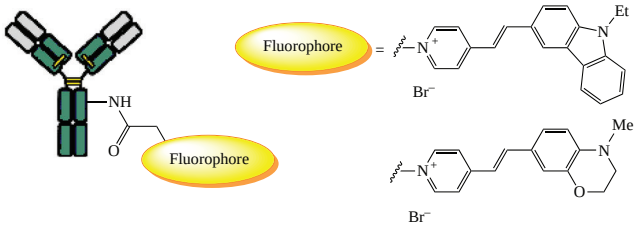

Keywords: fluorescent probes, covalent labeling, antibody, protein, styryl dyes, pyridinium salts.

Fluorescent labeling, a valuable field in biology and medicine, employs fluorescent markers, which allows detailed studies of various molecular mechanisms.[1–4] Nowadays, antibodies labeled with fluorophores are the most commonly used reagents in cell and molecular biology[5,6] for imaging, immunoassays, flow cytometry, Western blotting, and immunoprecipitation.[7–9]

In this study, styryl dyes containing the pyridinium cation as an acceptor and the carbazole or 3,4-dihydro-2*H*-1,4-benzoxazine fragment as a donor were chosen as fluorophore fragments. Carbazole derivatives are used as fluorescent probes to study DNA molecules,[10] proteins and enzymes,[11,12] cardiovascular compartments,[13,14] and other supramolecular assemblies.[15] 3,4-Dihydro-2*H*-1,4-benzoxazine stilbene-type compounds have not been previously described although their more hydrophilic structure may be useful in bioimaging.

Styryl dyes **1a**,**b** were prepared as shown in Scheme 1. Quaternization of 4-methylpyridine with *tert*-butyl 5-bromovalerate gave 4-methylpyridinium salt **3** whose methyl group was subjected to the Knoevenagel condensation with the corresponding aldehydes to afford intermediate products **2a**,**b**. Acids **1a**,**b** were synthesized in quantitative yields by removing the *tert*-butyl protection; intermediates **2a**,**b** were hydrolyzed by boiling in water in the absence of any catalyst. New compounds **1a**,**b**, **2a**,**b**, and **3** were identified and characterized by NMR spectroscopy, mass spectrometry, and elemental analysis (see Online Supplementary Materials).

The absorption spectra of derivatives **1a** and **1b** in an aqueous medium demonstrate broad bands at 423 and 446 nm, respectively (Figure 1), which correspond to intramolecular charge transfer from the electron-donating heterocyclic nitrogen atom to the electron-withdrawing pyridinium part. The dyes show a large Stokes shift and weak fluorescence in an aqueous medium (see Online Supplementary Materials, Table S1), which originate from the dominance of nonradiative relaxation of the excited state.[16,17]

It is known that the ICT-systems (ICT is intramolecular charge transfer) would demonstrate the solvatochromic effect.[16,17] The optical properties of dyes **1a** and **1b** were investigated in ten different solvents, including six protic and four aprotic ones, when the values of fluorescence quantum yields (φ^{fl}) and Stokes shift were determined (see Online Supplementary Materials, Table S1 and Figures S1–S4). The absorption maxima of dyes **1a** and **1b** in alcohols are mainly shifted hypsochromically with increasing solvent polarity. Such negative solvatochromism is observed when the ground state is more polar than the excited state. The fluorescence maxima

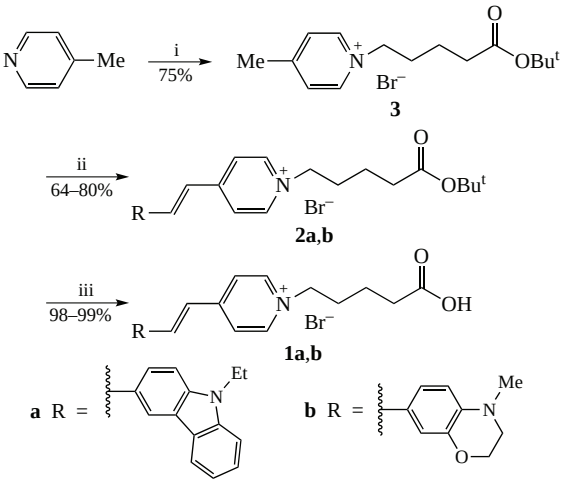

Scheme 1 *Reagents and conditions*: i, $Br(CH_2)_4CO_2Bu^t$, MeCN, 80 °C, 12 h; ii, RCHO, piperidine (cat.), Bu^nOH, 110 °C, 8 h; iii, H_2O, 100 °C, 24 h.

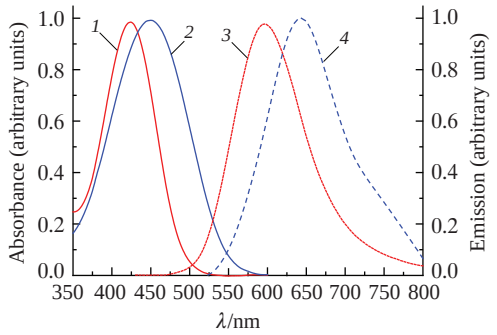

Figure 1 Absorption spectra for compounds (*1*) **1a** and (*2*) **1b**, and emission spectra for (*3*) **1a** and (*4*) **1b**. The spectra for **1a** and **1b** are shown by red and blue lines, respectively; $C_{\mathbf{1a},\ \mathbf{1b}} = 2.5 \times 10^{-6}$ mol dm^{-3}; H_2O; $\lambda_{ex,\ \mathbf{1a}} = 420$ nm; and $\lambda_{ex,\ \mathbf{1b}} = 480$ nm.

usually shift to the red region with increasing solvent polarity. The similar trends in λ_{abs} and λ_{fl} were reported for some analogous styryl dyes.[18]

On the basis of the obtained data, we plotted the Stokes shifts as a function of the solvent polarity factor – the orientation polarizability of the solvents Δf using the Lippert–Mataga equation (for details, see Online Supplementary Materials, page S13). A linear correlation between $\Delta\nu$ and Δf in protic solvents were observed (Figure 2). In the MeOH-*n*-$C_6H_{13}OH$ rank, the correlation coefficients are equal to 0.9871 and 0.9222 for compounds **1a** and **1b**, respectively. Water and decanol drop out of the obtained dependence, probably due to the presence of specific interactions with dyes. For aprotic solvents, no strict linear correlation was observed. Changes in the dipole moments of dyes **1a** and **1b** upon transition to an excited state were determined from the value of the tangent of the slope of the straight lines. The calculated values of $\mu_e - \mu_g$ are equal to 17.71 and 13.26 D for compounds **1a** and **1b**, respectively. Similar values were found in the literature for charged stilbenes.[19,20]

The dependence of the fluorescence quantum yield (φ^{fl}) of the dyes on the dynamic viscosity of the solvent is outlined in Figure 3. For compound **1b**, as the viscosity increases from 0.55 mPa s in methanol to 11.8 mPa s in decanol, a significant

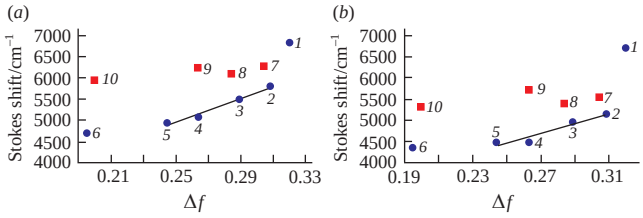

Figure 2 Stokes shifts for (*a*) compound **1a** and (*b*) compound **1b** as a function of solvent polarity. The solid line is the linear regression. Round markers stand for protic solvents: (*1*) H_2O, (*2*) MeOH, (*3*) EtOH, (*4*) *n*-BuOH, (*5*) *n*-$C_6H_{13}OH$, and (*6*) *n*-$C_{10}H_{21}OH$. Square markers stand for aprotic solvents: (*7*) MeCN, (*8*) acetone, (*9*) DMSO, and (*10*) EtOAc.

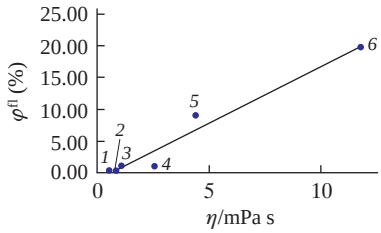

Figure 3 Fluorescence quantum yield φ^{fl} for compound **1b** as a function of dynamic viscosity η in: (*1*) H_2O, (*2*) MeOH, (*3*) EtOH, (*4*) *n*-BuOH, (*5*) *n*-$C_6H_{13}OH$, and (*6*) *n*-$C_{10}H_{21}OH$.

increase in the fluorescence intensity was observed. The increase in the fraction of radiative relaxation occurs due to the difficulty of free rotation in the molecule. Dye **1a** did not show a linear dependence of φ^{fl} on η in this viscosity range. A similar result was obtained for aprotic solvents. The absence of striking changes is explained by the narrow range of viscosity changes in the studied series.

To analyze the potential applicability of compounds **1a** and **1b** for protein labeling, we conjugated the dyes to antibodies and tested them in cytometric and microscopic tasks. For labeling an antibody specific to the Her2/neu tumor marker (Trastuzumab), the carboxy group of the dyes was activated in an aqueous medium by sulfo-*N*-hydroxysuccinimide (sulfo-NHS) in the presence of water soluble carbodiimide, 1-ethyl-3-(3-dimethylaminopropyl)carbodiimide (EDC), at pH 6. The resulting NHS ester was then added to the protein at pH 8 without isolation, and the conjugation product was purified by gel filtration. The labeling degree was ~1 and 2 dye per antibody for **1a** and **1b**, respectively. The lower availability of compound **1a** for labeling is probably caused by its higher hydrophobicity. Trastuzumab labeled with the green fluorescent dye AlexaFluor488 (AF488, 2 dyes per antibody) was used as a positive control. The obtained antibodies were incubated with EMT-HER2 cells (EMT6/P cells modified to express HER2) and control HeLa cells not carrying the target receptor. Cytometric analysis showed that the dye-

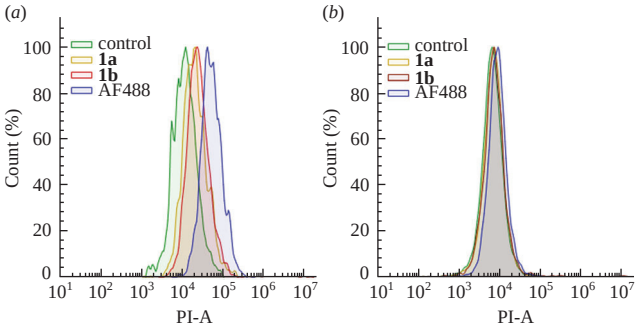

Figure 4 Results of cytometric analysis of (*a*) EMT-HER2 cells and (*b*) HeLa cells labeled with Trastuzumab-dye conjugates. Histograms for the PI channel are presented.

Table 1 Values of median fluorescence intensities of EMT-HER2 cells labeled with Trastuzumab-dye conjugates. Values relative to control cells in the same channel are given in parentheses.

Dye	Channel				
	488-nm laser[a]			405-nm laser[a]	
	530/30[b]	615/20[b]	660/20[b]	586/20[b]	615/20[b]
	FITC	PI	PerCP	Pacific Orange	Qdot 605
Control	7469 (1×)	11415 (1×)	10943 (1×)	9796 (1×)	20676 (1×)
1a	20683 (**2.8**×)	20020 (1.8×)	17622 (1.6×)	20347 (2.1×)	41744 (2.0×)
1b	8940 (1.2×)	24048 (2.1×)	29475 (**2.6**×)	12064 (1.2×)	28325 (1.4×)
AF488	314885 (42×)	51641 (4.5×)	25415 (2.3×)	12349 (1.3×)	25417 (1.2×)

[a] Excitation laser. [b] Transmission maximum and full width at half maximum of the emission filter in the channel.

labeled antibodies exhibit selective binding to HER2-positive cells (Figure 4). However, one can see that as compared to the control antibodies with AF488, antibodies with **1a** and **1b** showed a lower increase in signal relative to untreated cells (Table 1). This is fairly expected, taking into account the low quantum yield of the dyes in an aqueous medium. Due to the wide emission maximum and the large Stokes shift, dye **1a** was visible when excited by both blue (405 nm) and cyan (488 nm) lasers. Dye **1b** showed the best contrast in the PerCP channel (excitation at 488 nm and detection of emission at 660 nm). When excited with a blue laser (405 nm), the dyes demonstrated low contrast, probably due to a higher level of cell autofluorescence. Thus, the obtained styryl dyes can be used in cytometric applications; due to the large Stokes shift, they can 'occupy' non-standard channels, but the low brightness of the dyes in an aqueous medium restricts the sensitivity.

Next, we evaluated the potential applicability of dyes **1a** and **1b** in confocal scanning microscopy. We carried out imaging of EMT-HER2 cells with antibodies labeled with dyes **1a** and **1b** as well as with control antibodies labeled with AF488. Cells were readily stained with antibodies [Figure 5(*a*)], but, as in the case with cytometry, the signal from antibodies labeled with **1a** and **1b** was significantly lower. To evaluate the optimal spectral range of dye detection, we used a Zeiss LSM-980 microscope equipped with a detector acquiring data simultaneously in 32 channels in the range of 400–700 nm [Figure 5(*b*)]. It can be seen that the emission maxima are located at about 550 and 625 nm for **1a** and **1b**, respectively. These values are lower than the emission maxima of the dyes in solution, which can be explained by a decrease in the sensitivity of detectors with increasing wavelength of the detected light. Due to an unusually large Stokes shift, dye **1a** and especially dye **1b** should be well separated from standard green fluorophores such as Fluoresceine or AlexaFluor488. This is important in multiplexing experiments when several dyes are used.

In conclusion, dyes **1a** and **1b** exhibit a large Stokes shift and luminescence in the green-red region. Such dyes can be used for fluorescence labeling of proteins and subsequent fluorescence imaging or for use in cytometric tasks despite low fluorescence quantum yields in an aqueous medium. Further structure optimization involving blocking of the chromophore in forms with minimal conformational freedom can improve the brightness of the dyes.

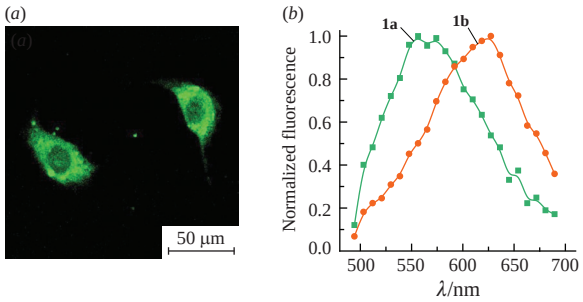

Figure 5 (*a*) EMT-HER2 cells after staining with Trastuzumab-dye **1a** conjugate as an example. (*b*) Emission of the cells labeled with Trastuzumab-dye conjugates in different detection spectral ranges measured by a multichannel microscope detector (excitation at 488 nm).

Synthesis and optical research were supported by the Ministry of Science and Higher Education of the Russian Federation (contract/agreement no. 075-00697-22-00) and were performed employing the equipment of the Center for Molecular Composition Studies of INEOS RAS. Cell culture, cytometry and microscopy experiments were supported by the Russian Science Foundation (grant no. 19-73-20194).

Online Supplementary Materials

Supplementary data associated with this article can be found in the online version at doi: 10.1016/j.mencom.2023.04.027.

References

1 V. I. Martynov, A. A. Pakhomov, N. V. Popova, I. E. Deyev and A. G. Petrenko, *Acta Naturae*, 2016, **8** (4), 33.
2 V. I. Martynov and A. A. Pakhomov, *Russ. Chem. Rev*., 2021, **90**, 1213.
3 V. E. Shershov, V. E. Kuznetsova, R. A. Miftakhov, S. A. Lapa, A. A. Stomahin, E. N. Timofeev, I. V. Grechishnikova, A. S. Zasedatelev and A. V. Chudinov, *Mendeleev Commun*., 2021, **31**, 70.
4 I. A. Doroshenko, K. G. Aminulla, V. N. Azev, T. M. Kulinich, V. A. Vasilichin, A. A. Shtil and T. A. Podrugina, *Mendeleev Commun*., 2021, **31**, 615.
5 A. H. Coons and M. H. Kaplan, *J. Exp. Med*., 1950, **91**, 1.
6 M. R. Dyson, Y. Zheng, C. Zhang, K. Colwill, K. Pershad, B. K. Kay, T. Pawson and J. McCafferty, *Anal. Biochem*., 2011, **417**, 25.
7 R. E. Cunningham, *Methods Mol. Biol*., 2010, **588**, 319.
8 S. L. Eaton, M. L. Hurtado, K. J. Oldknow, L. C. Graham, T. W. Marchant, T. H. Gillingwater, C. Farquharson and T. M. Wishart, *J. Visualized Exp*., 2014, e52099.
9 M. Dundas, D. Demonte and S. Park, *Appl. Microbiol. Biotechnol*., 2013, **97**, 9343.
10 X.-F. Zhang, H.-J. Zhang, J.-F. Xiang, Q. Li, Q.-F. Yang, Q. Shang, Y.-X. Zhang and Y.-L. Tang, *J. Mol. Struct*., 2010, **982**, 133.
11 R. Krieg, A. Eitner, W. Günther, C. Schürer, J. Lindenau and K.-J. Halbhuber, *J. Mol. Histol*., 2008, **39**, 169.
12 J. N. Wilson, A. S. Brown, W. M. Babinchak, C. D. Ridge and J. D. Walls, *Org. Biomol. Chem*., 2012, **10**, 8710.
13 F. Meng, Y. Liu, J. Niu and W. Lin, *RSC Adv*., 2017, **7**, 16087.
14 F. Miao, W. Zhang, Y. Sun, R. Zhang, Y. Liu, F. Guo, G. Song, M. Tian and X. Yu, *Biosens. Bioelectron*., 2014, **55**, 423.
15 H. Yin, F. Dumur, Y. Niu, M. M. Ayhan, O. Grauby, W. Liu, C. Wang, D. Siri, R. Rosas, A. Tonetto, D. Gigmes, R. Wang, D. Bardelang and O. Ouari, *ACS Appl. Mater. Interfaces*, 2017, **9**, 33220.
16 Z. R. Grabowski, K. Rotkiewicz and W. Rettig, *Chem. Rev*., 2003, **103**, 3899.
17 M. A. Haidekker and E. A. Theodorakis, *J. Biol. Eng*., 2010, **4**, 11.
18 A. Bajorek, K. Trzebiatowska, B. Jędrzejewska, M. Pietrzak, R. Gawinecki and J. Pączkowski, *J. Fluoresc*., 2004, **14**, 295.
19 B. Carlotti, G. Consiglio, F. Elisei, C. G. Fortuna, U. Mazzucato and A. Spalletti, *J. Phys. Chem. A*, 2014, 1**18**, 3580.
20 Y. Guo, C. S. Abeywickrama, D. Huo, J. Kong, M. Tao, A. Xia, Y. Pang and Y. Wan, *J. Phys. Chem. C*, 2020, **124**, 8550.

Received: 12th December 2022; Com. 22/7067